DOI: 10.1002/ejic.200700015

Preparation and Characterization of Dinuclear Ni^{II} Amine-Thiophenolate Complexes Coligated by EO_4^- (E = Cl, Re) and EO_4^{2-} Oxoanions (E = S, Cr, Mo, W)

Vasile Lozan[a] and Berthold Kersting*[a]

Keywords: Dinuclear complexes / Macrocyclic ligands / Oxoanions

The ability of dinuclear nickel(II) complexes of the type $[(L^{Me})Ni^{II}_2(L')]$ to coordinate tetrahedral main group and transition metal oxoanions ($L' = EO_4^-$, EO_4^{2-}) has been examined ($(L^{Me})^{2-}$ is the deprotonated form of the 24-membered macrocyclic hexaaza-dithiophenolate ligand H_2L^{Me}). The following complexes have been synthesized: $[(L^{Me})Ni_2(ClO_4)][ClO_4]$ (**2**$[ClO_4]$), $[(L^{Me})Ni_2(ReO_4)][ReO_4]$ (**3**$[ReO_4]$), $[(L^{Me})Ni_2(SO_4)]$ (**4**), $[(L^{Me})Ni_2(CrO_4)]$ (**5**), $[(L^{Me})Ni_2(MoO_4)]$ (**6**), and $[(L^{Me})Ni_2(WO_4)]$ (**7**). Complexes **2**$[ClO_4]$, **3**$[ReO_4]$, **4**, **5**, and **7** have been characterized by X-ray crystallography. The complexes are isostructural, with the EO_4^- and EO_4^{2-} groups bonded in a $\mu_{1,3}$-bridging mode to generate dioctahedral $N_3Ni(\mu\text{-}S)_2(\mu_{1,3}\text{-}EO_4)NiN_3$ core structures. The doubly charged EO_4^{2-} groups interact more strongly with the $[(L^{Me})Ni_2]^{2+}$ fragment than the EO_4^- groups as reflected by the Ni–O distances which are significantly longer in **2** and **3** than in **4**–**7**. The nickel(II) ions in **4** and **6** are weakly ferromagnetically coupled (J = 24.8 and 3.75 cm^{-1}, respectively) and the magnitude of the coupling appears to correlate with the Ni–S–Ni angle.

Introduction

The macrocyclic hexaaza-dithiophenolate macrocycle H_2L^{Me} is an effective dinucleating ligand that supports the formation of bioctahedral complexes of the type $[(L^{Me})M_2(L')]^+$ with numerous transition metals such as Mn, Fe, Co, Ni, Zn,[1] and Cd (Scheme 1).[2] These complexes have a rich coordination chemistry since the $[(L^{Me})M_2]^{2+}$ fragments are able to coordinate a large variety of coligands L′. These include Cl^-,[3] OH^-,[4] NO_2^-, NO_3^-, N_3^-,[5] BH_4^-,[6] various carboxylates,[7–9] N_2H_4, pyrazolate, and pyridazine,[5] and some biologically relevant molecules such as HCO_3^-, $(p\text{-}NO_2C_6H_4O)_2PO_2^-$, and proline.[10]

In earlier work, we have also described the synthesis of a few $[(L^{Me})M_2(L')]^+$ complexes bearing tetrahedral main group and transition metal oxoanions. The X-ray crystal structures of the complexes $[(L^{Me})Co^{II}_2(MoO_4)]$[11] and $[(L^{Me})Ni^{II}_2(O_2P(OH)_2)]^+$ have been reported.[7] In view of the biological, technological and environmental importance of these anions,[12,13] we considered it worthwhile to prepare further complexes of this type to gain more insight into the binding of the oxoanions by the $[(L^{Me})M_2]^{2+}$ fragments. Here we describe the synthesis and characterization of a series of novel dinickel complexes bearing ClO_4^-, ReO_4^-, SO_4^{2-}, CrO_4^{2-}, MoO_4^{2-}, and WO_4^{2-} ligands and explore their structural features.

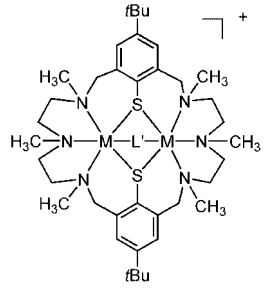

$[(L^{Me})M^{II}_2(L')]^+$
M = Mn, Fe, Co, Ni, Zn
L' = coligand

Scheme 1. Dinuclear $[(L^{Me})M_2(L')]^+$ complexes supported by the N_6S_2 macrocycle $(L^{Me})^{2-}$.

Results and Discussion

Synthesis of Complexes

The complexes were prepared as indicated in Scheme 2. The perchlorato (**2**) and perrhenato (**3**) complexes were found to be inaccessible by direct reactions of the chloro complex **1** and the respective EO_4^- ligand. In order to achieve their coordination, a Cl^- abstraction was necessary. When **1**$[ClO_4]$ was dissolved in CH_3CN and one equiv. of $Pb(ClO_4)_2$ was added, a dark green solution of **2** formed

[a] Institut für Anorganische Chemie, Universität Leipzig
Johannisallee 29, 04103 Leipzig, Germany
Fax: +49-341-97-36199
E-mail: b.kersting@uni-leipzig.de
Supporting information for this article is available on the WWW under http://www.eurjic.org or from the author.

immediately, from which the previously reported perchlorate salt **2**[ClO_4] could be isolated as a dark-green, air-stable solid.[6] The ClO_4^- in **2** is extreme labile and proved to be a suitable precursor for the synthesis of other $[(L^{Me})Ni_2(L')]^+$ complexes. Upon treatment of **2** with a large excess of [nBu$_4$N][ReO_4] in acetonitrile, both the ClO_4^- ligand and the ClO_4^- counterion can be substituted for ReO_4^- to give **3**[ReO_4], as indicated by elemental analyses and IR spectroscopy. Attempts to exchange the ClO_4^- ion by a MnO_4^- ion did not meet with any success. Treatment of **2**[ClO_4] with [nBu$_4$N][MnO_4] resulted in the formation of an insoluble brown solid, from which no products could be isolated.

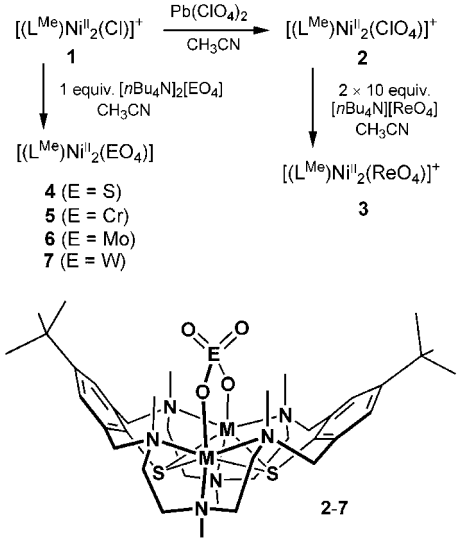

Scheme 2. Synthesis of complexes **2**–**7** from precursor **1**.

Although the Cl^- complex **1** proved to be less labile than the ClO_4^- complex **2**, substitution reactions succeeded with the EO_4^{2-} ions (E = S, Cr, Mo, W); the driving force behind these syntheses presumably being the low solubility of the resulting neutral complexes. Thus, when solutions of $[(L^{Me})Ni^{II}_2(Cl)]^+$ **1** in acetonitrile were treated with equimolar amounts of the respective [nBu$_4$N]$_2$[EO_4] salt at room temperature, pale green (**4**, **6**, **7**) or yellow (**5**) $[(L^{Me})Ni_2(EO_4)]$ complexes were formed within 4–12 h in good yields (69–88%). In contrast to **2**[ClO_4] and **3**[ReO_4], these neutral complexes were found to be sufficiently soluble in CH_2Cl_2, acetone, DMF, THF, but virtually insoluble in CH_3CN and MeOH. All complexes were characterized by elemental analysis and standard spectroscopic methods. The crystal structures of **2**[BPh_4]·1.5Me_2CO·0.5MeOH, **3**[ReO_4]·H_2O, **4**·2H_2O·MeCN, **5**, and **7**·2H_2O·MeCN were also determined by X-ray diffraction.

Spectroscopic Characterization

Infrared data for the complexes and their assignments are listed in Table 1. In addition to the bands arising from the $[(L^{Me})Ni_2]^{2+}$ fragments, all the complexes show strong IR bands for the $[EO_4]^{2-}$ and $[EO_4]^-$ groups. For the sulfato complex **4** two such bands are observed, as in other SO_4^{2-} complexes,[14] at 1120 and 620 cm^{-1}; these are assigned to the antisymmetric stretching (ν_3) and bending (ν_4) modes of the sulfate ion. In view of the lowering of the symmetry by coordination to the $[(L^{Me})Ni_2]^{2+}$ fragment, a splitting of the ν_3 mode of the $[EO_4]^{2-}$ ion is expected.[15] For **4** and **5**, this splitting is not resolved. In the case of the molybdato and wolframato complexes **6** and **7**, however, a split ν_3 band is clearly discernible. Each of these compounds reveals two nearly equally intense absorptions in the 800 to 850 cm^{-1} range, typical for coordinated $[MoO_4]^{2-}$,[14] and $[WO_4]^{2-}$ groups.[16] The IR spectra of **2**[ClO_4] and **3**[ReO_4] both reveal two broad but unsplit bands reflecting the presence of coordinating and non-coordinating EO_4^- species. The observed wavenumbers are not markedly different from those of the free ions.[17–19]

The electronic spectra of the compounds were registered in acetonitrile or dichloromethane solution. Selected data are reported in Table 1. The intense absorptions below 500 nm can be attributed to π-π* transitions within the aromatic rings of the supporting ligand or to $RS^-\rightarrow Ni^{II}$ charge-transfer bands. Above 500 nm, each compound displays two weak absorption bands, typical of six-coordinate nickel(II) complexes.[20,21] Both the ν_1 and the ν_2 transitions are broad and unsymmetrical, indicative of the presence of a significant distortion from octahedral symmetry. The

Table 1. Selected spectroscopic data for complexes **2**–**7**.

	IR[a] $\tilde{\nu}_3$ [cm^{-1}]	$\tilde{\nu}_4$ [cm^{-1}]	UV/Vis[b] λ_{max} [nm] (ε, $M^{-1}cm^{-1}$)
Free ClO_4^- [17,18]	1100	620	–
Free ReO_4^- [19]	920	322	–
Free SO_4^{2-} [14]	1105	611	–
Free CrO_4^{2-} [19]	890	368	–
Free MoO_4^{2-} [14]	841	338	–
Free WO_4^{2-} [16]	833	324	–
$[(L^{Me})Ni_2(ClO_4)]^+$ **2**	1097, 1113	624	578 (129), 1066 (86)
$[(L^{Me})Ni_2(ReO_4)]^+$ **3**	931, 903	–	670 (79), 1058 (127)
$[(L^{Me})Ni_2(SO_4)]$ **4**	1120	620	674 (16), 1122 (34)
$[(L^{Me})Ni_2(CrO_4)]$ **5**	895	–	686 (79), 1126 (88)
$[(L^{Me})Ni_2(MoO_4)]$ **6**	854, 817	–	690 (104), 1136 (142)
$[(L^{Me})Ni_2(WO_4)]$ **7**	857, 820	–	689 (1132), 1132 (130)

[a] IR spectra were recorded as KBr pellets. [b] The UV/Vis spectra were recorded in MeCN (**2**, **3**) or CH_2Cl_2 solution (for **4**–**7**) at ambient temperature.

slight differences in the position of the *d-d* transitions show that each complex retains its integrity in solution. The solid state magnetic moments for **4** and **6** are also consistent with an octahedral structure (see below).

X-ray Crystallography

From a solution of the perchlorate salt of **2** in acetone/methanol to which $NaBPh_4$ had been added, pale green crystals of **2**$[BPh_4]\cdot 1.5Me_2CO\cdot 0.5MeOH$ suitable for X-ray crystallographic analysis were obtained after slow evaporation. The structure consists of dinuclear nickel complexes, tetraphenylborate anions, and acetone and methanol molecules of solvent of crystallization. There are no intermolecular interactions between these components in the solid state. Figure 1 presents an ORTEP view of the cation **2**. Selected bond lengths and angles are given in Table 2 and Table 3. The cation is isostructural with the other nickel complexes, with the perchlorate being coordinated in a bidentate bridging mode and the supporting ligand adopting a bowl-shaped C_{2v} symmetric conformation typical for $[(L^{Me})M^{II}_2(L')]$ complexes coligated by $\mu_{1,3}$-bridging oxyanions.[22] The lability of the perchlorato complex is reflected in the long Ni–O bonds at 2.144(6) Å. In fact, this is the longest Ni–O distance reported for dinuclear $[(L^{Me})Ni_2(L')]^+$ complexes. Note, that the elongation of the Ni–O bonds in **2** is compensated for by an increase of the Ni–N and Ni–S distances. Overall, these structural parameters indicate that the monocharged perchlorate ion binds more weakly to the dinuclear $[(L^{Me})Ni_2]^{2+}$ fragment in **2** than does the doubly charged sulfato ligand in **4**.

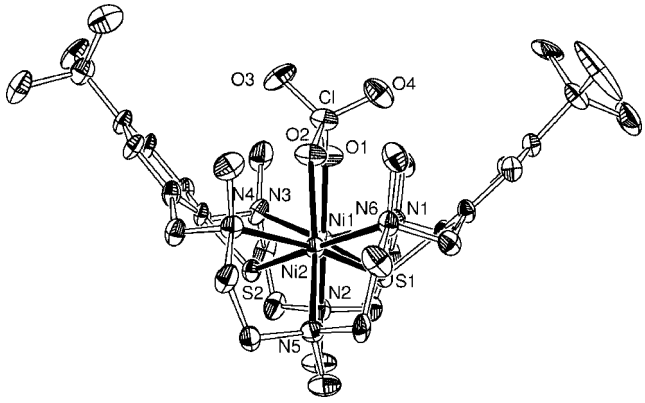

Figure 1. Structure of the cation **2** in crystals of **2**$[BPh_4]\cdot 1.5Me_2CO\cdot 0.5MeOH$. Thermal ellipsoids are drawn at the 30% probability level. Hydrogen atoms are omitted for reasons of clarity.

Pale green crystals of the perrhenato complex **3**$[ReO_4]\cdot H_2O$ suitable for X-ray diffraction analysis were obtained by slow evaporation of an acetonitrile/ethanol solution. The crystal structure consists of the dinuclear perrhenate complex **3**, perrhenate anions and water solvate molecules. As can be seen from Figure 2, complex **3** is isostructural with **2**. Within the $[(L^{Me})Ni_2]^{2+}$ fragments in **2** and **3**, the Ni–S and Ni–N bond lengths are very similar, with the largest difference outside experimental error being ca. 0.1 Å in the Ni–N(6) bonds. The coordination of the larger perrhenate group also results in a slight opening up of the Ni–S–Ni angles to 94.95(7)° thereby causing a larger Ni···Ni separation of 3.630(1) Å. The Ni–O distances are slightly shorter than in **2**, but still larger than those in **4** and **7**. In contrast to **2**, the terminal oxygen atoms of the two ReO_4^- groups are involved in hydrogen bonding interactions with the water molecule of solvent of crystallization. These hydrogen bonds may be classified as moderate based on the bond

Table 2. Selected bond lengths [Å] in complexes **2**–**4** and **7**.

	2 (E = Cl)	**3** (E = Re)	**4** (E = S)	**7** (E = W)
Ni(1)–O(1)	2.122(6)	2.091(5)	2.001(2)	2.000(4)
Ni(1)–N(1)	2.245(7)	2.219(5)	2.221(3)	2.220(5)
Ni(1)–N(2)	2.114(7)	2.114(5)	2.185(3)	2.168(5)
Ni(1)–N(3)	2.248(7)	2.258(6)	2.339(3)	2.305(5)
Ni(1)–S(1)	2.433(2)	2.499(2)	2.461(1)	2.498(2)
Ni(1)–S(2)	2.467(2)	2.434(2)	2.483(1)	2.505(2)
Ni(2)–O(2)	2.165(5)	2.110(5)	2.017(3)	2.000(4)
Ni(2)–N(4)	2.277(7)	2.206(5)	2.231(3)	2.229(5)
Ni(2)–N(5)	2.136(6)	2.132(6)	2.165(3)	2.153(5)
Ni(2)–N(6)	2.172(7)	2.267(5)	2.298(3)	2.269(5)
Ni(2)–S(1)	2.434(3)	2.456(2)	2.441(1)	2.454(2)
Ni(2)–S(2)	2.462(2)	2.462(2)	2.533(1)	2.572(2)
Ni–N[a]	2.198(7)	2.199(6)	2.240(3)	2.224(5)
Ni–O[a]	2.144(6)	2.101(5)	2.009(2)	2.000(4)
Ni–S[a]	2.449(3)	2.463(2)	2.480(1)	2.507(2)
M(1)···M(2)	3.547(1)	3.630(1)	3.506(1)	3.655(1)
M(1)···E	3.379(1)	3.564(1)	3.263(1)	3.491(1)
M(2)···E	3.403(1)	3.563(1)	3.298(1)	3.532(1)
E–O(1)	1.446(5)	1.722(5) [1.703(7)][b]	1.488(3)	1.763(4)
E–O(2)	1.451(5)	1.729(5) [1.716(7)][b]	1.485(3)	1.772(4)
E–O(3)	1.444(7)	1.702(7) [1.705(6)][b]	1.447(3)	1.749(4)
E–O(4)	1.407(7)	1.710(6) [1.698(6)][b]	1.461(3)	1.778(5)
E–O[a]	1.437(7)	1.716(6) [1.706(7)][b]	1.470(3)	1.766(4)

[a] Average values. [b] Values in square brackets refer to the ReO_4^- counteranion.

Table 3. Selected bond angles [°] in complexes **2**, **3**, **4** and **7**.

	2	**3**	**4**	**7**
N–M–N[a]	88.7(3)	89.6(2)	87.8(1)	89.3(2)
N–M–S[a]	95.2(2)	94.7(2)	94.16(9)	94.0(1)
O–M–N_{cis} [a]	86.2(3)	85.0(2)	87.3(1)	85.8(2)
O–M–S_{cis} [a]	93.9(2)	96.3(2)	96.10(8)	97.9(1)
S–M–S[a]	77.96(8)	76.42(6)	78.35(4)	75.74(6)
O–M–N_{trans} [a]	162.6(3)	161.2(2)	162.3(1)	160.4(2)
N–M–S_{trans} [a]	168.6(2)	166.9(2)	168.22(9)	165.9(1)
M–S–M[a]	92.80(9)	94.95(7)	90.00(4)	93.61(6)
O(1)–E–O(2)	108.6(3)	106.5(2)	109.59(15)	106.5(2)
O(1)–E–O(3)	108.6(4)	110.7(3)	109.35(17)	110.9(2)
O(1)–E–O(4)	109.1(4)	110.1(3)	108.50(17)	109.6(2)
O(2)–E–O(3)	109.5(4)	112.4(3)	109.71(18)	109.6(2)
O(2)–E–O(4)	109.8(4)	109.0(3)	109.11(18)	111.9(2)
O(3)–E–O(4)	111.1(5)	108.1(4)	110.6(2)	108.3(2)

[a] Average values.

lengths of ca. 2.8 Å [O(4)···O(9) 2.822 Å, O(6)···O(9) 2.842 Å]. Similar hydrogen-bonding interactions are also observed in **4** and **7**.

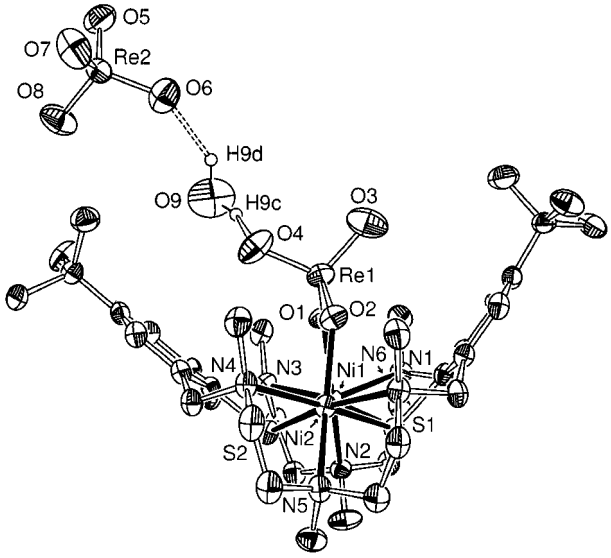

Figure 2. ORTEP plot of the structure of **3**. The hydrogen bonding interactions between the water molecule and the perrhenate groups are shown (dashed lines). Thermal ellipsoids are drawn at the 30% probability level. Hydrogen atoms, except H(9c) and H(9d), are omitted for reasons of clarity.

Pale green crystals of the sulfato complex **4**·2H_2O·MeCN were grown by slow evaporation of a mixed (1:1) ethanol/acetonitrile solution of **4**. Figure 3 provides an ORTEP view of the structure of the neutral complex. As in **3**, there is a short O···O distance between the sulfato oxygen atom O(4) and a water molecule [*d*(O(4)···O(5) 2.671 Å] indicative of a hydrogen-bonding interaction. Complex **4** is the first example of a [(L^{Me})Ni_2(L′)] complex bearing a doubly charged coligand. A comparison of structure **2** with structure **4** allows the effects of ClO_4^- vs. SO_4^{2-} coordination in otherwise identical [(L^{Me})Ni_2]$^{2+}$ fragments to be evaluated. The only significant differences among these complexes are in the average Ni–O bond lengths, with the sulfato complex having significantly shorter Ni–O bonds than the perchlorato complex, most likely as a consequence of an increased electrostatic interaction. In this regard, it is also interesting to note that the terminal S=O bonds are slightly shorter than the bridging S–O bonds [e.g., 1.454(3) vs. 1.487(3) Å]. A similar behaviour has been noted previously for [(L^{Me})-Co^{II}_2(MoO_4)].[11]

Slow evaporation of a CH_2Cl_2 solution of the chromato complex **5** gave orange crystals that were analyzed by X-ray crystallography. Although, the structure determination is of low quality and not as good as desired for publication,[23] it can serve to confirm the formulation and the atom connectivity of the neutral CrO_4^{2-} complex. The structure is depicted in Figure 4, but not discussed further.

The wolframato complex **7** is isomorphous with **4**, with very similar unit cell parameters and molecular dimensions. The molecular structure is illustrated in Figure 5, and salient bond lengths and angles are given in Table 2 and

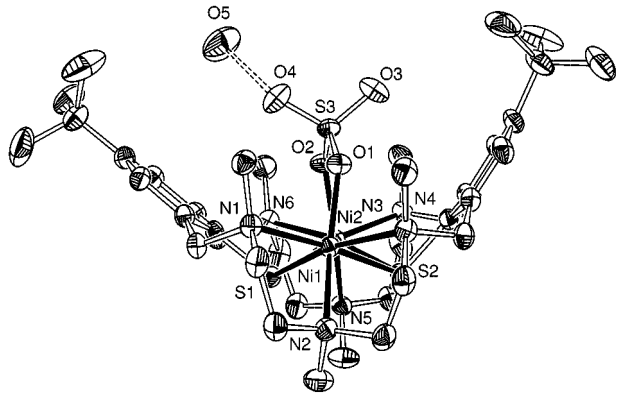

Figure 3. ORTEP plot of the neutral complex **4**. Thermal ellipsoids are drawn at the 30% probability level. Hydrogen atoms are omitted for reasons of clarity. The dashed line indicates the hydrogen bond between the sulfato oxygen atom O(4) and the water molecule O(5).

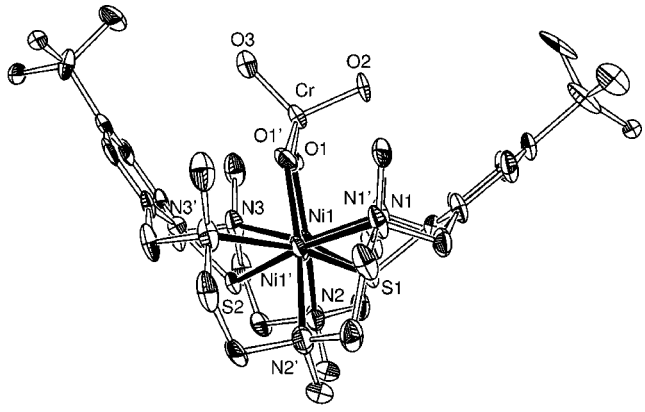

Figure 4. Structure of the neutral complex **5** with thermal ellipsoids drawn at the 50% probability level. Hydrogen atoms are omitted for reasons of clarity. Only one orientation of the disordered *t*Bu groups is displayed. Selected bond lengths [Å] and angles [°]: Ni–O(1) 2.001, Cr–O(1) 1.671, Cr–O(2) 1.639, Cr–O(3) 1.644; Ni(1)–S(1)–Ni(1′) 94.3, Ni(1)–S(2)–Ni(1′) 89.3. Symmetry code used to generate equivalent atoms: *x*, 0.5–*y*, *z* (′).

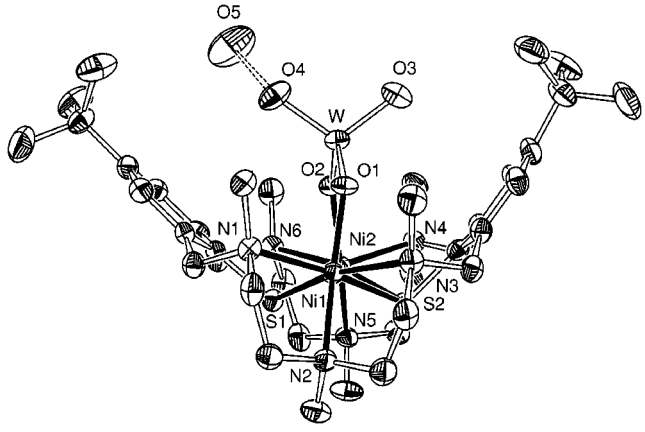

Figure 5. ORTEP plot of complex **7**. Thermal ellipsoids are drawn at 50% probability. Hydrogen atoms have been omitted for reasons of clarity. The dashed line indicates the hydrogen bond between the wolframato oxygen atom O(4) and the water molecule O(5).

Table 3. The average Ni–O bond length of 2.000(4) Å resembles that in **4**, again much shorter than in **2** and **3**. In agreement with the splitting of the v_3 band in the IR, the coordination about the tungsten atom is not perfectly tetrahedral. The W–O bonds vary between 1.749(4) Å and 1.778(4) Å and the O–W–O bond angles range from 106.5(2) to 111.9(2)°. The Ni···Ni separation is 3.655(1) Å in **7** and is 3.506(1) in **4**. As a consequence, the Ni–S–Ni bond angle in the wolframato complex **7** (93.61(6)°] is wider than in **4** (90.00(4)°].

Magnetic Properties of Complexes 4 and 6

Temperature-dependent magnetic susceptibility measurements for complexes **4** and **6** were carried out to see whether magnetic exchange interactions are present in these complexes. The temperature dependent susceptibility data for powdered samples of the two complexes have been measured between 4.0 and 289 K by using a Faraday balance in an applied external magnetic field of 1.1 T. Figure 6 displays the temperature dependence of the effective moment (μ_{eff} per dinuclear complex) for complex **4**. The effective magnetic moment increases from 4.58 μ_B at 295 K to a maximum value of 5.10 μ_B at 25 K, and then decreases rapidly to 4.94 μ_B at 4.4 K. This behaviour indicates an intramolecular ferromagnetic exchange interaction between the two Ni^{II} ions that leads to an S = 2 ground state of complex **4**. The decrease in μ_B below 22 K is presumably due to zero-field splitting of Ni^{II}.

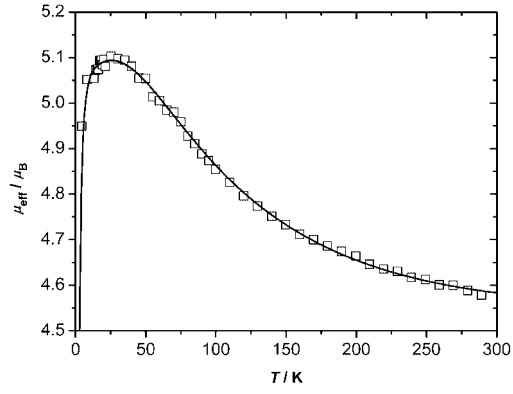

Figure 6. Temperature dependence of μ_{eff} for **4** (per dinuclear complex). The full line represents the best theoretical fit to eq. (1). Experimental and calculated values are provided as supporting information.

The temperature dependence of the magnetic moment for the wolframato complex **6** is similar to that of the sulfato complex **4** (Figure 7). The effective magnetic moment per dinuclear complex also increases from 4.33 μ_B at 295 K to a maximum of 5.08 μ_B at 10 K and then decreases again with decreasing temperature. The fact that the maximum occurs at lower temperatures than in **4** is indicative of a weaker ferromagnetic exchange interaction between the two Ni^{II} ions in **6**.

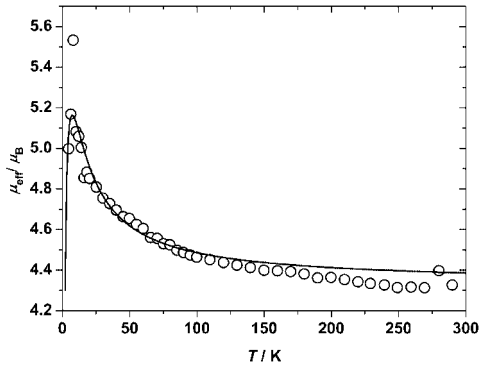

Figure 7. Temperature dependence of μ_{eff} for the molybdato complex **6** (per dinuclear complex). The full line represents the best theoretical fit to eq. (1). Experimental and calculated values are provided as supporting information.

To determine the magnitude of the exchange interactions, the temperature dependence of the magnetic data were simulated using the appropriate spin-Hamiltonian (1) including the isotropic HDVV exchange, the single-ion zero-field splitting and the single-ion Zeeman interaction by using a full-matrix diagonalization approach.[22,24] For complex **4** an excellent fit was obtained with J = +24.8 cm^{-1}, g = 2.08, and $|D|$ = 2.56 cm^{-1}. The experimental data for complex **6** were also analyzed in terms of the spin-Hamiltonian in eq. (1) The best fit gave J = +3.75 cm^{-1}, g = 2.17, and $|D|$ = 3.27 cm^{-1}. Although the experimental data could not be reproduced in every detail in this case, it is clear that the exchange interaction between the two Ni^{II} ions in **6** is also ferromagnetic in nature and that this interaction is significantly weaker than in **4**.

$$H = -2JS_1S_2 + \sum_{i=1}^{2}[D_i(\hat{S}_{zi}^2 - \tfrac{1}{3}S_i(S_i+1)) + g_i\mu_B S_i B] \qquad (1)$$

It has been noted previously, that there exists a relationship between the sign and magnitude of the coupling parameter and the Ni–S–Ni angle in bioctahedral dinickel complexes supported by $(L^{Me})^{2-}$.[5,22] The coupling is antiferromagnetic in nature if the Ni–S–Ni angle deviates by more than about ±10° from 90°. For angles within the 90 ± 10° range a ferromagnetic interaction is observed. Moreover, the closer the Ni–S–Ni angles is at 90° the higher will be the magnitude of the ferromagnetic exchange interaction. Our observations of ferromagnetic exchange interactions in **4** and **6**, for which the Ni–S–Ni angles are in the 90 ± 10° range,[25] are in good agreement with the reported trend.

Conclusions

The ability of the $[(L^{Me})Ni_2]^{2+}$ fragment to bind tetrahedral oxoanions of various main-group and transition elements has been demonstrated with the synthesis of a series of cationic (n = 1) and neutral complexes (n = 0) of the

type $[(L^{Me})Ni_2(EO_4)]^{n+}$, namely $[(L^{Me})Ni_2(ClO_4)]^+$ (**2**), $[(L^{Me})Ni_2(ReO_4)]^+$ (**3**), $[(L^{Me})Ni_2(SO_4)]$ (**4**), $[(L^{Me})Ni_2(CrO_4)]$ (**5**), $[(L^{Me})Ni_2(MoO_4)]$ (**6**), and $[(L^{Me})Ni_2(WO_4)]$ (**7**). All complexes were readily prepared and fully characterized by elemental analysis, IR and UV/Vis spectroscopy. The single-crystal X-ray structure determinations of **2**[BPh_4], **3**[ReO_4], **4**, **5**, and **7** showed the oxoanions to be coordinated in a $\mu_{1,3}$-bridging mode. Analysis of the structural parameters indicate that the monocharged EO_4^- ions bind more weakly to the dinuclear $[(L^{Me})Ni_2]^{2+}$ fragment in **2** and **3** than the doubly charged EO_4^{2-} groups in **4**–**7**. This was further confirmed by the lability of the ClO_4^- ion in **2**, which renders this complex to be a suitable starting material for other $[(L^{Me})Ni_2(L')]^+$ complexes. The binding and solubility differences of the cationic and neutral $[(L^{Me})Ni_2(EO_4)]$ complexes suggests a possible use of the $[(L^{Me})Ni_2]^{2+}$ fragment in the selective recognition or separation of tetrahedral oxoanions. Studies on these and related topics are in progress in our laboratory.

Experimental Section

All preparations were carried out under argon. Reagent grade solvents were used throughout. $[(L^{Me})Ni^{II}_2Cl]ClO_4$ (**1**) was prepared as described previously.[3] $[nBu_4N]_2[CrO_4]$ and $[nBu_4N]_2[MoO_4]$ were prepared from $[nBu_4N]OH$ and CrO_3 or $MoO_3{\cdot}2H_2O$,[26] respectively, using the procedure reported for $[nBu_4N]_2[WO_4]$.[27] All other reagents were obtained from standard commercial sources and used without further purifications. Melting points were determined in open glass capillaries and are uncorrected. Infrared spectra were recorded on a Bruker VECTOR 22 FT-IR spectrometer. The electronic absorption spectra were measured on a Jasco V-570 UV/Vis/NIR spectrometer. Elemental analyses were carried out with a VARIO EL elemental analyzer. Temperature-dependent (295–2 K) magnetic susceptibility measurements were carried out on Faraday balance (Manics DSM10 magnetometer) over the temperature range 4–295 K in an external magnetic field of 1.1 T. The observed susceptibility data were corrected for the underlying diamagnetism by the use of tabulated Pascal's constants.

Caution! *Perchlorate salts of transition metal complexes are hazardous and may explode. Only small quantities should be prepared and handled with great care.*

$[(L^{Me})Ni^{II}_2(\mu\text{-}ClO_4)][ClO_4]$ (2[ClO_4]): To a solution of $[(L^{Me})Ni^{II}_2Cl][ClO_4]$ (**1**[ClO_4]) (184 mg, 0.200 mmol) in MeCN (50 mL) was added solid $Pb(ClO_4)_2$ (44.7 mg, 0.110 mmol). The reaction mixture was stirred for 2 h before $PbCl_2$ was removed by filtration. To the dark green filtrate was added a solution of $LiClO_4{\cdot}3H_2O$ (321 mg, 2.00 mol) in EtOH (100 mL). The solution was concentrated in vacuo to afford a dark green precipitate which was isolated by filtration and dried in air. Yield: 148 mg (75%). M.p. 308–309 °C (decomp.). IR (KBr): $\tilde{\nu}$ = 3443 (s br), 3045 (w), 3024 (w), 2992 (w), 2958 (s), 2900 (w), 2866 (s), 2815 (w), 1489 (w), 1462 (s), 1426 (w), 1395 (m), 1377 (w), 1363 (m), 1345 (vw), 1326 (w), 1310 (m), 1293 (w), 1262 (m), 1236 (m), 1200 (w), 1170 (m), 1156 (s), 1113 [vs, $\nu_3(ClO_4^-)$], 1097 [vs, $\nu_3(ClO_4^-)$], 1019 (m), 1000 (w), 981 (w), 911 (m), 932 (m), 895 (w), 882 (m), 824 (s), 818 (s), 808 (w), 754 (w), 624 [s, $\nu_4(ClO_4^-)$], 603 (w), 564 (w), 544 (w), 533 (w), 494 (w), 418 (w) cm^{-1}. UV/Vis (MeCN): λ (ε, $M^{-1}cm^{-1}$) = 578 (129), 1066 (86) nm. $C_{38}H_{64}Cl_2N_6Ni_2O_8S_2{\cdot}EtOH{\cdot}H_2O$ (985.37 + 64.08): calcd. C 45.78, H 6.92, N 8.01, S 6.11; found C 46.06, H 6.82, N 8.06, S. 6.00.

$[(L^{Me})Ni^{II}_2(ReO_4)][ReO_4]$ (3[ReO_4]): To a solution of $[(L^{Me})Ni_2(ClO_4)][ClO_4]$ (98 mg, 0.100 mmol) in acetonitrile (30 mL) was added an acetonitrile solution (20 mL) of $[nBu_4N][ReO_4]$ (493 mg, 1.00 mmol). The mixture was stirred for 12 h and concentrated in vacuo to give a yellow solid, which was filtered, washed with ethanol and dried in air. To remove traces of perchlorate impurities this material was treated again with a ten-fold molar excess of $[nBu_4N][ReO_4]$ as described above. Recrystallization from a mixed ethanol/acetonitrile solvent system then gave the title compound in analytically pure form. Yield: 107 mg (81%). M.p. > 365 °C (decomp.). IR (KBr): $\tilde{\nu}$ = 3560 (m), 3465 (m), 2961 (s), 2867 (s), 2248 [w, ν(CN)], 1869 (w), 1637 (w), 1597 (w), 1461 (s), 1423 (w), 1394 (m), 1362 (m), 1306 (m), 1262 (m), 1231 (m), 1200 (w), 1168 (w), 1152 (m), 1132 (w), 1102 (w), 1074 (s), 1063 (s), 1041 (s), 998 (w), 977 (w), 963 (w), 931 [s, $\nu_3(ReO_4^-)$], 909 [s, $\nu_3(ReO_4^-)$], 824 (s), 807 (m), 751 (m), 666 (w), 630 (m), 602 (w), 564 (w), 539 (w), 531 (w), 493 (w), 467 (w), 434 (w), 416 (w) cm^{-1}. UV/Vis (CH_3CN): λ (ε, $M^{-1}cm^{-1}$) = 670 (79), 1058 (127) nm. $C_{38}H_{64}N_6Ni_2O_8Re_2S_2{\cdot}CH_3CN$ (1286.88 + 41.05): calcd. C 36.18, H 5.09, N 7.38, S 4.83; found C 36.81, H 5.22, N 7.44, S 5.00.

$[(L^{Me})Ni^{II}_2(SO_4)]$ (4): To a solution of $[nBu_4N][HSO_4]$ (0.17 mg, 0.50 mmol) in acetonitrile (50 mL) was added NEt_3 (50 mg, 0.50 mmol), followed by $[(L^{Me})Ni_2Cl][ClO_4]$ (184 mg, 0.200 mmol). The reaction mixture was stirred for 12 h to give a pale-green solid which was filtered, washed with methanol and dried in air. Yield: 129 mg (69%). M.p. 340–341 °C (decomp.). IR (KBr): $\tilde{\nu}$ = 3417 (s), 2962 (s), 2867 (s), 2091 (w), 1643 (m), 1461 (s), 1394 (w), 1362 (m), 1309 (w), 1263 (m), 1235 (m), 1202 (w), 1120 [s br, $\nu_3(SO_4^{2-})$], 1056 (s), 1041 (s), 999 (w), 984 (w), 931 (w), 912 (m), 879 (m), 825 (s), 818 (s), 754 (m), 651 (w), 629 (m), 620 [m, $\nu_4(SO_4^{2-})$], 564 (w), 543 (w), 493 (w), 446 (w), 416 (w) cm^{-1}. UV/Vis (CH_2Cl_2): λ (ε, $M^{-1}cm^{-1}$) = 674 (16), 1122 (34) nm. $C_{38}H_{64}N_6Ni_2O_4S_3{\cdot}3H_2O$ (882.53 + 54.05): calcd. C 48.73, H 7.53, N 8.97, S 10.27; found C 48.66, H 7.59, N 8.90, S 10.08.

$[(L^{Me})Ni^{II}_2(CrO_4)]$ (5): To a solution of $[nBu_4N]_2[CrO_4]$ (120 mg, 0.200) in acetonitrile (40 mL) was added $[(L^{Me})Ni_2Cl][ClO_4]$ (184 mg, 0.200 mmol). The reaction mixture was stirred for 4 h to give a yellow precipitate which was isolated by filtration, washed with acetonitrile, and dried in air. Yield: 134 mg (73%). M.p. 300–301 °C (decomp.). IR (KBr): $\tilde{\nu}$ = 3409 (s), 3045 (m), 2961 (s), 2866 (s), 1638 (m), 1604 (m), 1480 (s), 1460 (s), 1393 (s), 1362 (s), 1307 (m), 1265 (m), 1232 (m), 1202 (w), 1170 (w), 1153 (m), 1132 (w), 1110 (w), 1080 (s), 1060 (s), 1044 (s), 1000 (w), 981 (w), 895 [s, $\nu_3(CrO_4^{2-})$], 817 (s), 752 (m), 667 (w), 629 (s), 564 (w), 541 (w), 529 (w), 448 (w), 415 (w) cm^{-1}. UV/Vis (CH_2Cl_2): λ (ε, $M^{-1}cm^{-1}$) = 391 (1891), 686 (79), 1126 (88) nm. $C_{38}H_{64}CrN_6Ni_2O_4S_2{\cdot}H_2O$ (902.47 + 18.02): calcd. C 49.58, H 7.23, N 9.13, S 6.97; found C 49.31, H 6.89, N 9.54, S 6.52.

$[(L^{Me})Ni^{II}_2(MoO_4)]$ (6): To a solution of $[(L^{Me})Ni_2Cl][ClO_4]$ (92 mg, 0.100 mmol) in acetonitrile (40 mL) was added $[nBu_4N]_2[MoO_4]$ (129 mg, 0.200 mmol). The mixture was stirred for 12 h to give a green solid, which was filtered and dried in air. Yield: 86 mg (88%). M.p. 316–318 °C (decomp.). IR (KBr): $\tilde{\nu}$ = 3416 (s), 2953 (s), 2867 (s), 2248 (w), 2045 (w), 1639 (m), 1460 (s), 1393 (m), 1362 (m), 1306 (m), 1264 (m), 1231 (m), 1203 (w), 1170 (w), 1153 (m), 1131 (w), 1113 (w), 1079 (s), 1065 (s), 1044 (s), 1001 (w), 982 (w), 928 (m), 911 (m), 879 (m), 854 [s, $\tilde{\nu}_3(MoO_4^{2-})$], 817 [s, $\nu_3(MoO_4^{2-})$], 753 (m), 667 (w), 628 (m), 603 (w), 564 (w), 528 (w), 493 (w), 446 (w), 414 (w) cm^{-1}. UV/Vis (CH_2Cl_2): λ (ε, $M^{-1}cm^{-1}$) = 358 (2256), 690 (104), 1136 (142) nm. $C_{38}H_{64}MoN_6Ni_2O_4S_2{\cdot}2H_2O$ (946.41 + 36.03): calcd. C 46.46, H 6.98, N 8.55, S 6.53; found C 46.63, H 6.66, N 9.15, S 6.22.

Table 4. Crystallographic data for **2**, **3**, **4**, and **7**.

Compound	**2**[BPh_4]·1.5Me_2CO·0.5MeOH	**3**[ReO_4]·H_2O	**4**·2H_2O·MeCN	**7**·2H_2O·MeCN
Formula	$C_{67}H_{95}BClN_6Ni_2O_6S_2$	$C_{38}H_{66}N_6Ni_2O_9Re_2S_2$	$C_{40}H_{71}N_7Ni_2O_6S_3$	$C_{40}H_{71}N_7Ni_2O_6S_2W$
M_r [g/mol]	1308.29	1304.91	959.64	1111.43
Space group	$P\bar{1}$	$P\bar{1}$	$P2_1/c$	$P2_1/c$
a [Å]	15.820(6)	11.153(3)	13.681(2)	13.759(2)
b [Å]	16.171(5)	14.408(4)	19.196(3)	19.550(2)
c [Å]	16.769(5)	16.110(4)	17.814(2)	17.990(2)
α [deg]	64.85(2)	68.220(4)	90.00	90
β [deg]	72.37(2)	69.864(5)	102.91(3)	102.01(3)
γ [deg]	66.13(2)	78.117(4)	90.00	90
V [Å^3]	3506(2)	2248(1)	4560(1)	4735(1)
Z	2	2	4	4
$d_{calcd.}$ g/cm^3	1.239	1.928	1.398	1.559
Crystal size [mm^3]	0.42 × 0.35 × 0.20	0.30 × 0.30 × 0.20	0.20 × 0.20 × 0.20	0.26 × 0.20 × 0.18
μ(Mo-K_α) [mm^{-1}]	0.686	6.343	1.015	3.349
θ limits [deg]	1.36–28.77	1.42–28.87	1.58–28.85	1.56–28.88
Measured reflections	10580	19924	27855	17414
Independent reflections	10536	10343	10832	10583
Observed reflections[a]	4462	7529	7503	6872
Parameters	794	532	512	521
R_1[b] (R_1 all data)	0.0682 (0.1580)	0.0400 (0.0626)	0.0510 (0.0788)	0.0434 (0.0813)
wR_2[c] (wR_2 all data)	0.1772 (0.2165)	0.1158 (0.1272)	0.1576 (0.1752)	0.0993 (0.1156)
Max./min. peaks [e Å^3]	0.936/–0.818	2.085/–2.501	2.375/–1.079	1.409/–1.855
CCDC number	631192	631193	631194	631195

[a] Observation criterion: $I > 2\sigma(I)$. [b] $R1 = \Sigma||F_o| - |F_c||/\Sigma|F_o|$. [c] $wR2 = \{\Sigma[w(F_o^2 - F_c^2)^2]/\Sigma[w(F_o^2)^2]\}^{1/2}$.

[(L^{Me})Ni^{II}_2(WO_4)] (7): To a solution of [(L^{Me})Ni_2Cl][ClO_4] (92 mg, 0.100 mmol) in acetonitrile (40 mL) was added [$n$$Bu_4N$]$_2$[$WO_4$] (146 mg, 0.200 mmol). The mixture was stirred for 4 h to give a green solid, which was filtered and dried in air. Yield: 92 mg (86%). M.p. 318–320 °C (decomp.). IR (KBr): $\tilde{\nu}$ = 3399 (s), 2951 (s), 2867 (s), 1685 (m), 1647 (m), 1604 (m), 1459 (s), 1393 (m), 1362 (m), 1306 (w), 1262 (m), 1231 (m), 1203 (w), 1170 (w), 1153 (m), 1131 (w), 1112 (w), 1079 (s), 1065 (s), 1044 (s), 1001 (w), 979 (w), 928 (m), 911 (m), 898 (m), 880 (m), 857 [s, $\nu_3(WO_4^{2-})$], 818 [s, $\nu_3(WO_4^{2-})$], 753 (m), 667 (w), 628 (m), 604 (w), 563 (w), 542 (w), 528 (w), 493 (w), 447 (w), 414 (w) cm^{-1}. UV/Vis (CH_2Cl_2): λ (ε, M^{-1}cm^{-1}) = 689 (90), 1132 (130) nm. $C_{38}H_{64}N_6Ni_2O_4S_2W$·2$H_2O$ (946.41 + 36.03): calcd. C 42.64, H 6.40, N 7.85, S 5.99; found C 42.82, H 6.27, N 8.71, S 5.50.

Crystallography: Crystals of **2**[BPh_4]·1.5(Me_2CO)·0.5H_2O were obtained from an acetone solution of **2**[ClO_4] to which a solution of $NaBPh_4$ in methanol had been added. Single-crystals of **5** were grown by recrystallization from CH_2Cl_2. All other compounds crystallized upon slow evaporation from 1:1 acetonitrile/ethanol solutions. Crystal data and refinement details are listed in Table 4. The intensity data were collected on a Bruker Smart CCD diffractometer. Graphite-monochromated Mo-K_α radiation (λ = 0.71073 Å) was used throughout. The data were processed with SAINT[28] and corrected for absorption using SADABS.[29] The structures were solved by direct methods (SHELXS)[30] and refined by full-matrix least-squares on F^2 using SHELXTL (version 5.1).[31] All non-hydrogen atoms were refined with anisotropic displacement parameters, except the C and O atoms of the disordered MeOH molecule in **2**.

Some of the solvate molecules in **2**, **4** and **7** were found to be severely disordered and/or partially occupied. The MeOH molecule in **2** lies near an inversion center such that only half a molecule lies in the asymmetric unit. The occupancy factor of one acetone molecule was also reduced to 0.5, and the C and O atoms were refined with equivalent anisotropic thermal parameters. In addition, one *tert*-butyl group was found to be disordered over two positions. A split atom model with restrained C–C and C···C distances was applied by using appropriate SADI instructions. In the isomorphous complexes **4** and **7**, one water molecule was found to be disordered over two sites with occupation factors of ca. 0.7 and 0.3. The C and N atoms of the acetonitrile molecule in **7** reveal high displacement parameters indicative of disorder. It was not possible to resolve this disorder, and geometric constraints using DFIX instructions were required to keep the structure of the solvate molecule reasonable. The MeCN molecule in **4**·2H_2O·MeCN could not be located from Fourier maps. The coordinates of the atoms were taken from the structure of **7** and the acetonitrile molecule was allowed to ride on the oxygen atom O(6b) by using an AFIX 3 instruction. The hydrogen atoms were placed at calculated positions and refined as riding atoms with isotropic displacement parameters, e.g., U_{iso}(H) = 1.2 × U_{iso}(parent) or U_{iso}(H) = 1.5 × U_{iso}(C) for methyl groups. The hydrogen atoms of the water molecule in **3** were calculated assuming a O–H distance of 0.96 Å and an ideal tetrahedral geometry. For **4** and **7**, water and acetonitrile hydrogen atoms were not included in the refinement. Graphics were obtained with ORTEP 3 for Windows.[32]

CCDC-631192 to -631195 contain the supplementary crystallographic data for this paper. These data can be obtained free of charge from The Cambridge Crystallographic Data Centre via www.ccdc.cam.ac.uk/data_request/cif.

Supporting Information (see also the footnote on the first page of this article): Derivation of the magnetic susceptibility expression for **4** and **6** and magnetic susceptibility data for **4** and **5** as a function of the temperature.

Acknowledgments

This work was supported by the Deutsche Forschungsgemeinschaft (DFG) (KE 585/3-1,2,3). We are particularly grateful to Prof. Dr. H. Vahrenkamp for providing facilities for IR and X-ray crystallographic measurements.

[1] B. Kersting, *Z. Anorg. Allg. Chem.* **2004**, *630*, 765–780.
[2] V. Lozan, B. Kersting, *Eur. J. Inorg. Chem.* **2005**, 504–512.
[3] B. Kersting, G. Steinfeld, *Chem. Commun.* **2001**, 1376–1377.
[4] M. H. Klingele, G. Steinfeld, B. Kersting, *Z. Naturforsch., Teil B* **2001**, *56*, 901–907.
[5] J. Hausmann, V. Lozan, M. H. Klingele, G. Steinfeld, D. Siebert, Y. Journaux, J. J. Girerd, B. Kersting, *Chem. Eur. J.* **2004**, *10*, 1716–1728.
[6] Y. Journaux, J. Hausmann, V. Lozan, B. Kersting, *Chem. Commun.* **2006**, 83–84.
[7] B. Kersting, *Angew. Chem.* **2001**, *113*, 4110–4112; *Angew. Chem. Int. Ed.* **2001**, *40*, 3988–3990.
[8] B. Kersting, G. Steinfeld, *Inorg. Chem.* **2002**, *41*, 1140–1150.
[9] G. Steinfeld, V. Lozan, B. Kersting, *Angew. Chem.* **2003**, *115*, 2363–2365; *Angew. Chem. Int. Ed.* **2003**, *42*, 2261–2263.
[10] B. Kersting, G. Steinfeld, unpublished results.
[11] V. Lozan, B. Kersting, *Inorg. Chem.* **2006**, *45*, 5630–5634.
[12] J. Nelson, V. McKee, R. M. Town in *Macrocyclic Chemistry, Current Trends and Future Perspectives*, K. Gloe (Eds.), Springer, Berlin, **2005**.
[13] *Supramolecular Chemistry of Anions* (Eds.: A. Bianchi, K. Bowman-James, E. Garcia-Espana), Wiley-VCH, New York, **1997**.
[14] R. Coomber, W. P. Griffith, *J. Chem. Soc. A* **1968**, 1128–1131.
[15] K. Nakamoto, *Infrared and Raman Spectra of Inorganic and Coordination Compounds*, 5th ed., part B; VCH-Wiley, New York, **1997**, p. 79ff.
[16] A. Thiele, J. Fuchs, *Z. Naturforsch., Teil B* **1979**, *34*, 145–154.
[17] M. D. Santana, A. Rufete, G. Garcia, G. Lopez, J. Casabo, A. Cabrero, E. Molins, C. Miravitlles, *Polyhedron* **1997**, *16*, 3713–3721.
[18] M. Yonemura, Y. Matsumura, H. Furutachi, M. Ohba, H. Okawa, D. E. Fenton, *Inorg. Chem.* **1997**, *36*, 2711–2717.
[19] N. Weinstock, H. Schulze, A. Müller, *J. Chem. Phys.* **1973**, *59*, 5063–5067.
[20] A. McAuley, S. Subramanian, *Inorg. Chem.* **1990**, *29*, 2830–2837.
[21] K. R. Adam, M. Antolovich, D. S. Baldwin, L. G. Bridgen, P. A. Duckworth, L. F. Lindoy, A. Bashall, M. McPartlin, P. A. Tasker, *J. Chem. Soc., Dalton Trans.* **1992**, 1869–1876.
[22] Y. Journaux, T. Glaser, G. Steinfeld, V. Lozan, B. Kersting, *Dalton Trans.* **2006**, 1738–1748.
[23] Preliminary data of the crystal structure determination of **5**: $C_{38}H_{64}CrN_6Ni_2O_4S_2$, M_r = 902.49, orthorhombic, space group *P*nma, a = 26.91(4), b = 12.30(2), c = 12.84(2) Å, V = 4250(13) Å^3, Z = 4, μ(Mo-K_a) = 1.27 mm^{-1}, $\rho_{calcd.}$ = 1.410 g cm^{-3}, R = 0.18 for 5310 reflections with $I > 2\sigma(I)$.
[24] B. Kersting, G. Steinfeld, D. Siebert, *Chem. Eur. J.* **2001**, *7*, 4253–4258.
[25] The average Co–S–Co angle in [(L^{Me})$Co_2(MoO_4)$] is at 90.75°, see ref.[10]. We assume that the Ni–S–Ni angles in **4** is also larger in than 90°. We estimate it to be ca. 93° based on the structure of **7**.
[26] G. Brauer, *Handbuch der Präparativen Anorganischen Chemie*, vol. 3, Ferdinand Enke Verlag, Stuttgart, **1981**, p. 1544.
[27] W. Clegg, R. J. Errington, K. A. Fraser, D. G. Richards, *J. Chem. Soc., Chem. Commun.* **1993**, 1105–1107.
[28] *SAINT+*, V6.02, Data Reduction and Frame Integration Program for the CCD Area-Detector System, Bruker AXS, Madison, WI, **1999**.
[29] G. M. Sheldrick, *Program SADABS:* Area-detector absorption correction.
[30] G. M. Sheldrick, *Acta Crystallogr., Sect. A* **1990**, *46*, 467–473.
[31] G. M. Sheldrick, *SHELXTL NT 5*.10, Bruker AXS, Bruker AXS, Madison, WI, **1998**.
[32] a) L. J. Farrugia, ORTEP 3 for Windows, Version 1.05, University of Glasgow, **1997**; L. J. Farrugia, *J. Appl. Crystallogr.* **1997**, *30*, 565.

Received: January 5, 2007
Published Online: February 22, 2007

